10B.4

Processes involved in the Planetary Boundary Layer in the frame of the West African Monsoon

Marie Lothon* (1), Guylaine Canut(1), Frédérique Saïd(1), Françoise Guichard(2), Fleur Couvreux(2), Fabienne Lohou(1) and Bernard Campistron(1)

(1) Université de Toulouse, Laboratoire d'Aérologie - CNRS UMR 5560, Toulouse, France
(2) Centre National de Recherche Météorologique, Météo-France, Toulouse

1. INTRODUCTION

Although generated and ruled at the global scale, the West African Monsoon shows a very striking diurnal cycle through most of its components (Peyrillé and Lafore (2007), Parker et al. (2005)) : the thermal heat low in the Saharian desert (Lavaysse et al., 2008), the Inter Tropical Front (ITD)—lower interface of the moist southwesterly monsoon flow and the dry saharian air— (Lothon et al., 2008). Even the African Easterly Jet, thermal wind at around 500 hPa produced by the temperature gradient between the West African continental surface and the Atlantic Ocean to the south, shows a diurnal cycle (Lee et al., 2007) in addition to periodicities of a 3-4 days associated with the African Easterly Waves (AEW) (Burpee, 1972) and larger periods.

This is due to the strong role played by the surface-atmosphere interaction within the WAM system and the very large contrasts of surface from the north of the region to the south. As an interface between the surface and the free atmosphere, the planetary boundary layer (PBL) is inherently involved in the processes of the WAM diurnal cycle. The Sahel is of special interest in the context of the WAM, because of its sensitivity in various ways—from climate, hydrology, agriculture, economy, health to sociology—, due to its location at the transition between vegetated areas to the south (Benin, Togo, Nigeria) and the desert to the north (Niger, Mali, Algeria).

The diurnal oscillation of the low troposphere in this area is manifested by a low level jet in the night (Lothon et al., 2008) and a deep PBL developing during the day for most of the year. However, during the wettest months, both dry convection and nocturnal jet are weakened, and deep convection takes place instead. Depending on the position of the ITD, which shows a seasonal migration northward before the monsoon onset and southward for its retreating (Sultan et al., 2007), the wind in the lower layers is easterly (dry season) or southwesterly (wet season).

Here we use observations of 15 flights during the AMMA (African Monsoon Multidisciplinary Analysis) Special Observing Periods (SOP) that took place during the summer of 2006 (Lebel et al., 2007) to study the PBL structure in this area and context and its role in the WAM. We especially focus on the nature of the interaction between the moist monsoon flow and the overlying dry Saharian Air Layer (SAL) through PBL processes and transports, in the transition time of the monsoon setting (dry or shallow cumulus convection, troposphere moistening), and during its active phase when deep convection occurs.

2. DATASET

In Fig. 1, the water vapor mixing ratio observed at the ground at Niamey (13°29'N, 2°10'E, 205 m a.s.l.) during the entire year 2006 shows how marked the seasons are in this area, with very dry air from November to mid April, moistening during 2 to 3 months before a quite short wet season in August and September, and a short drying transition in October. During the dry season, the ITD is south to the area, and the wind at the ground is the northeasterly wind locally called 'Harmattan'.

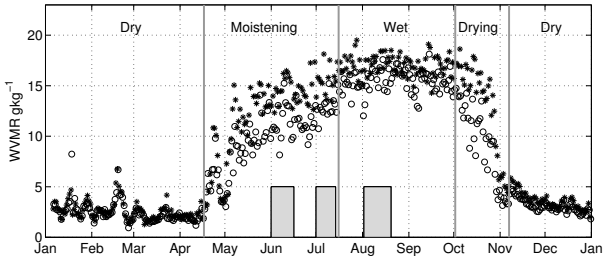

Figure 1: *(*) Night-time and (○) daytime averaged water vapor mixing ratio measured at surface at Niamey airport in 2006. Shaded area stand for SOPs considered here.*

The moistening transition starts when the ITD has crossed the area in its migration northward. The wind at the ground can be either monsoon—which progressively moistens the low troposphere—or Harmattan (ususally during the day, in the first part of that period). The abrupt shift of the Intertropical Convergence Zone (ITCZ) put into

*corresponding author address: Marie Lothon, Centre de Recherches Atmosphériques, 8 route de Lannemezan, 65300 Campistrous, France; *email*: lotm@aero.obs-mip.fr

evidence by Sultan and Janicot (2000) sets the start of the active phase of the monsoon. The water vapor mixing ratio in Niamey is maximum then and leveled.

Here we focus only on the three periods indicated by the shaded areas in Fig. 1, which correspond to SOPs when the ATR research aircraft flew in the low and mid-troposphere. During all those periods, the ITD is located north to Niamey and the flow in the lowest part of the troposphere is the monsoon flow most of the time.

During AMMA, the ATR aircraft flew intensively in the lower troposphere in the vicinity of Niamey area, with instruments that allow fast measurements of wind, temperature and humidity. 60- to 80-km stacked legs flown within and above the PBL, both into the moist southwesterly monsoon flow and the dry north-easterly flow of the SAL allowed us to characterize the vertical structure of the PBL and study the exchanges between the two opposite flows. Eight flights made before the monsoon onset, from early June to mid-July, and seven flights made during the active phase of the monsoon between early August and mid-August are considered in our analysis.

We applied a 5-km filter to the 25 s^{-1} time series to remove the mesoscale variability that cannot be sampled correctly and introduces errors into the calculation of fluxes. After a close comparison of filtered and unfiltered series, their resulting turbulent moments, and a calculation of the systematic and random errors (based on Lenschow et al. (1994)), we found that the results shown here do not change when considering either filtered or unfiltered series. The turbulent moments were calculated on 5- to 7.5-minute segments, that is from 30 to 45 km long.

We also use the measurements of the UHF wind profiler and of radiosounding operated by the Aerosol Radiation Measurements (ARM) facility at Niamey airport during all year 2006. During the SOPs, 4 radiosoundings were launched per day, at about 0000, 0600, 1200 and 1800 UTC.

The 5-beam 915 MHz wind profiler gives profiles of wind and reflectivity at 5 min interval with a vertical resolution of 60 m up to 2.4 km a. g. l. at low mode. A 25 min average is applied for the data shown here. We can obtain estimates of the structure coefficient of the refractive index C_n^2, which is proportional to the reflectivity. During the day, it is usually maximum at the top of the PBL. During the night, its high values can reveal the strong gradients of humidity and large wind shear.

The airport was situated about 50 km away from the area usually probed by the aircraft, which was often centered around Banizoumbou, where turbulent, radiation and aerosol measurements were made during AMMA.

All the flights (8) flown before the monsoon onset were made over Banizoumbou. After the onset, the flying area depended on where the convective systems were forecasted and/or where it rained. But we considered only the flights that were less than 100 km away from Niamey.

3. DIURNAL CYCLE OF THE LOWER LAYERS IN THE WAM

Figure 2 shows a 24h sequence of horizontal wind and C_n^2 vertical profiles observed by the UHF wind profiler of Niamey airport for the 11 June. This is about one month and half that the ITD passed the area northward, and the monsoon flow is established (southerly or southwesterly wind). It is increased during the night in a low level jet with a maximum at about 400 m a. g. l. of about 12 ms^{-1} windspeed.

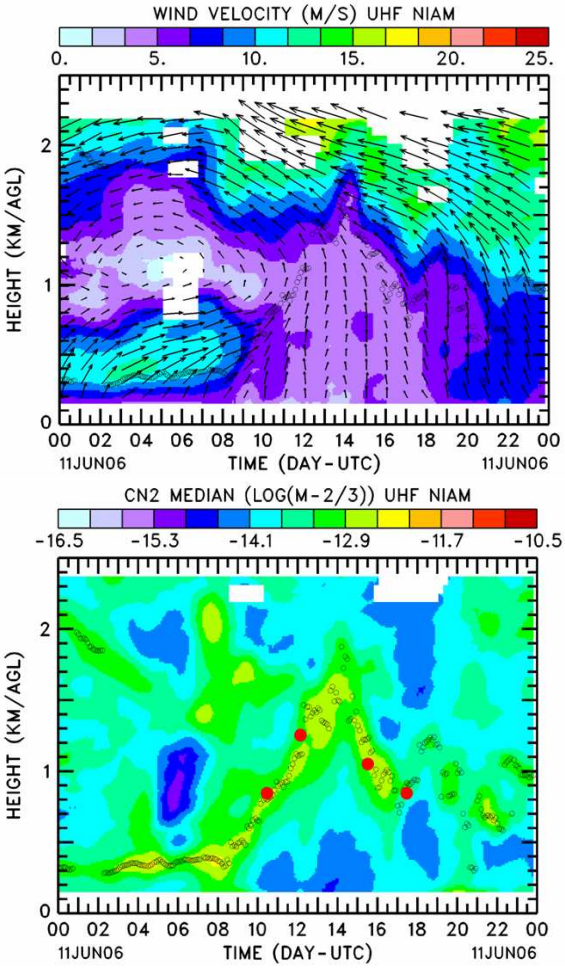

Figure 2: *Height-time cross section of (top) horizontal wind (arrows for direction and speed and colorscale for windspeed) and (bottom) structure coefficient of the refractive index C_n^2. An arrow that is pointing toward the top in the top panel indicates a southerly wind. The circles indicate estimates of z_i based on (black) C_n^2 maximum or (red) radiosoundings.*

In the contrary, dry convection during the day lightens

the wind by mixing. As seen in Fig. 2, the PBL deepens quickly after eroding the nocturnal jet and its top can reach 2000 m (bottom panel) to 3000 m in other days.

The soundings in Fig. 3 show that the nocturnal jet brings water vapor every night by advection, and the vertical turbulent transport redistributes it vertically during the day. By the end of the morning, the PBL top z_i has often reached the shear zone between the monsoon flow and the SAL, which favours the exchanges between the two opposite flows and the PBL growth. It results in an efficient drying of the lowest layers and a moistening of the lower part of the SAL in the mid-troposphere.

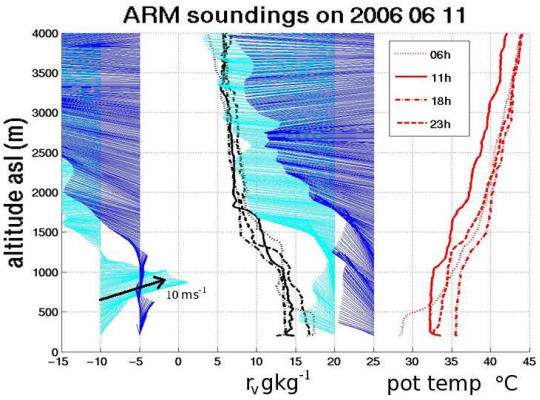

Figure 3: *Soundings made at Niamey airport on 11 June, at 0600, 1100, 1800 and 2300 UTC. The x-axis indicates both the water vapor mixing ratio in gkg^{-1} (black lines) and the potential temperature in °C (red lines). The wind profiles are plotted chronologically from left to right.*

The diurnal cycle as described above is typical of this moistening transition (see Fig. 1). A little bit earlier, when the ITD is close to the area (this was at the end of April and early May in Niamey in 2006), the diurnal cycle is still more striking, because the westerly nocturnal jet is stronger then (Sultan et al. (2007) and Lothon et al. (2008)) and the dry convection during the day mixes the SAL/monsoon interface enough to make the ITD retreat southward, and the northeasterly Harmattan wind is observed at the ground and into the PBL during the day instead of the monsoon flow. The PBL can be quite deep then, up to 4000 m.

Still earlier, during the dry season that is long in Niamey, the ITD is more to the south and the whole troposphere is dry and occupied by easterly wind of the SAL and Harmattan at the ground. The PBL is deep and dry.

During the wet season, the frequent deep convection events, the moister ground and troposphere, result in a much weaker diurnal cycle and thinner PBL (its depth is about 1000 m deep all along the wet season). However, the nocturnal jet can still settle during some nights.

The aircraft observations shown here were obtained (1) during the moistening transition mentioned before (first two shaded periods in Fig. 1), with more and more water vapor advected to the north, and increasing chances for moist convection that manifest themselves by the enhanced presence of shallow cumulus clouds in July and (2) during the wetter period. Most of the flights were made at midday, to reduce the non-stationarity of the conditions. They allowed us to describe the processes involved in the vertical redistribution of water by turbulence mixing. Though the second period is much more complicated by the presence and large role played by the clouds, as a first approach of the issue here, we intend to see the changes in our results from the first period to the active phase of the monsoon.

4. SMALL SCALE SUBSIDENT DRY TONGUES AND IMPACT ON THE PBL STRUCTURE

Figure 4 shows examples of the fluctuations in vertical air velocity w, potential temperature θ, and water vapor mixing ratio r_v that can be measured right above or right below the PBL top in the first period of observations (note that we drop the prime usually used for fluctuations to simplify the notation). Those are evidences of the exchanges between the PBL and the much dryer and warmer SAL above. θ and r_v can be very much correlated when the aircraft crossed some dry parcels coming from above the PBL top, as seen in this figure, and they usually are associated with negative w, even if the latter is not as much correlated with the two scalars.

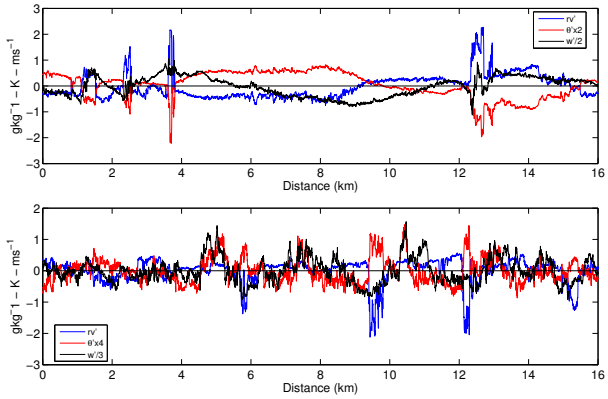

Figure 4: *High rate time series of the fluctuations in w (black line), θ (red) and r_v (blue) during part of one leg flown (top) slightly above the PBL top on 5 June and (bottom) right below the PBL on 6 June. Note the different scaling used for w and θ.*

This reveals the process of entrainment of those dry and warm parcels, indirectly with the pushing upward thermals that drive the air from above across the inversion by suction. The impact of similar dry tongues were

studied previously by Couvreux et al. (2005) (see also Couvreux et al. (2007) with LES in the context of IHOP experiment (Weckwerth et al., 2004) and observed during Hapex by Lothon et al. (2007)). They are a few hundred meters large and a few km apart, as seen in Fig. 4.

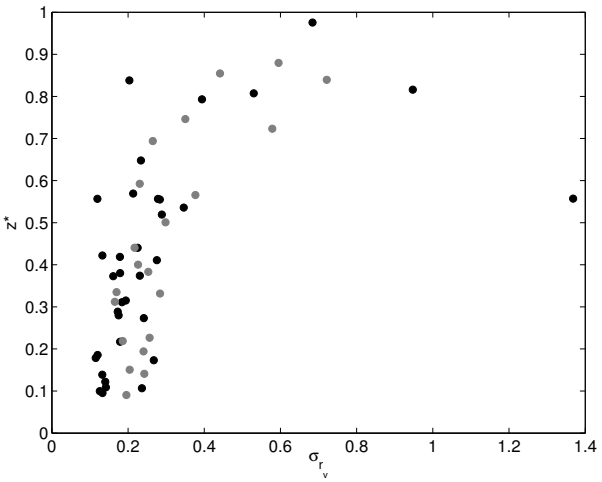

Figure 5: *r_v standard deviation as a function of normalized height, observed during (black) 8 flights made before the monsoon onset and (gray) 7 flights made after.*

r_v standard deviation associated with those subsident dry tongues is quite large in the upper part of the PBL, as shown in Fig. 5. The profile also shows that they are still present during the wet phase. The resulting profiles of heat fluxes are quite specific, as displayed in Fig. 6. During the first period especially, the latent heat flux is around zero close to surface due to dryness, and the flux is large at the PBL top due to the dry subsident tongues. The latent heat flux profiles in Fig. 6 are normalized by the flux at the top for the first period in order to emphasis on the linear increasing flux from zero up to a maximum at the top that could reach about 500 Wm^{-2}. During the wet period, the latent heat flux is not zero anymore at surface, and the vertical profile observed can be either increasing or decreasing depending on the entrainment flux at the top (the profiles are normalized by the surface latent heat flux for the second period). The latent heat flux profiles are linear most of the time, but less than the sensible heat flux profiles. The sensible heat flux profile are also often largely negative at the top, because of the larger potential temperature of the dry tongues relative to the PBL environment. The profiles of sensible heat are all normalized by the surface flux in Fig. 6. They are rigorously linear.

Another characteristic of the PBL vertical structure associated with the subsident dry tongues is the negative skewness of the water vapor (Fig. 7), as found previously by Couvreux et al. (2007) in the Great Plains. It is mini-

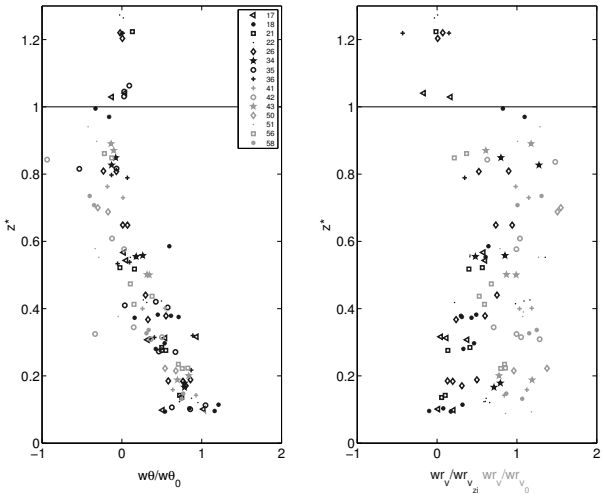

Figure 6: *Vertical profiles of (left panel) sensible heat and (right panel) latent heat flux, (black) before and (gray) after the onset. The sensible heat fluxes are normalized by the surface flux. The latent heat fluxes are normalized by the entrainment flux during the first period, and by the surface flux during the second period.*

mum around 0.4 z_i, with skewness down to less than -1. During the second period, r_v skewness is less negative and can become positive close to surface due to moister ground and significant latent heat flux in the surface layer (around 200 to 400 Wm^{-2}). It can also be positive at the top, probably due to the clouds. But it is still negative in the middle of the PBL.

In order to characterize the scales associated to the dry tongues, we arbitrarily define the dry tongues with the following procedure: we look for fluctuations for which $w < 0$, $\theta > 0$ and $r_v < -1.5\ \sigma_{r_v}$. This is similar to what is typically done to characterize thermals (see i. e. Lenschow and Stephens, 1980) or what was done by Nicholls (1989) for the study of entrainment in marine stratocumulus. From this, we deduce the number of dry intrusions per entire leg (60 to 80 km long). Their width l is obtained from the number of datapoints with $r_v < 0$ around the selected peak and the distance between them D is defined as the distance between the centers of the dry tongues detected that way. In average, we find that l = 400 $\pm$ 80 m and remains constant between the first and second period, while D = 2000 m $\pm$ 400 m during the moistening period and larger (2400 m) during the wet period (with less detected intrusions). We also find similar distributions of D and l to those found by Miao and Geerts (2006) for thermals in the convective boundary-layer. Normalized by the PBL depth, D and l are very well correlated (Fig. 8), especially during the first period, and we find that the distance between the dry tongues is about 6 times larger than their width. This ratio of course

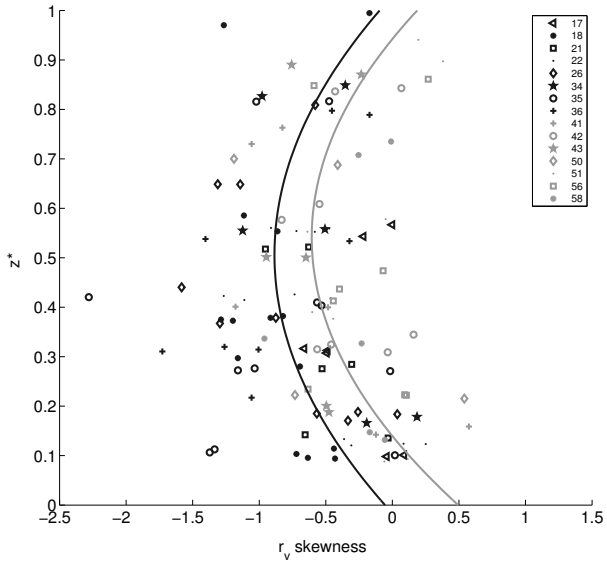

Figure 7: *Vertical profiles of r_v skewness, (black) before and (gray) after the onset.*

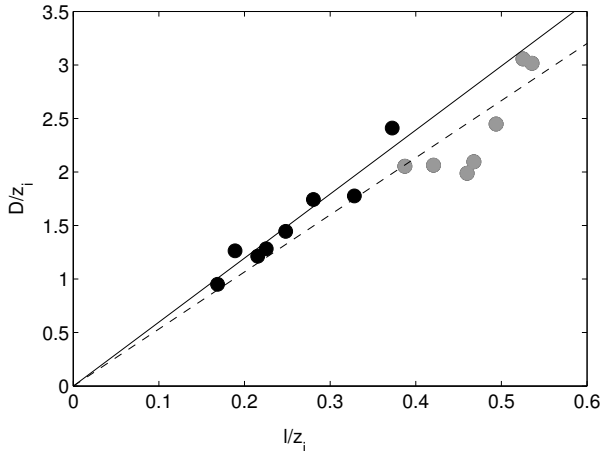

Figure 8: *Normalized distance between dry tongues as a function of normalized width, (black) before and (gray) after the onset.*

depends on the definition criteria, but remains around that order, which is close to that observed for thermals (Miao and Geerts, 2006). During the second period, D is close to 2.4 z_i while it is about 2 z_i during the first period. The correlation between distance and width is also less strong.

We find that increasing the threshold of $1.5\ \sigma_{r_v}$ to detect the intrusions, or low-filtering the series, makes D and l larger as one can expect, but does not change the ratio between both. However, calling dry intrusions what we detect in the second period may be close to the edge, because they are much less obvious: the smaller standard deviation makes the detection threshold smaller too and the occurrence of dry tongues still large with this way to proceed. We plan to define the detection threshold based on the water vapor jump across the inversion rather than from the standard deviation observed in the considered leg in order to evaluate how sensitive the characteristics that we find are to the criteria used to define them.

We also estimated the contribution of the dry tongues in the fluxes and variances relative to the thermals, by carrying out a conditional analysis on w, θ and r_v. Considering a dry intrusions as having $w < 0$ and $r_v < 0$ and the thermals as having $w > 0$ and $\theta > 0$, we found that the contribution of the dry tongues to fluxes and variances could reach 40 to 60% at the PBL top and be prevailing down to 0.6 z_i. From surface to 0.4 z_i, thermals are predominant. Those two classes play the largest role in the sahelian PBL structure.

5. ENTRAINMENT AT THE PBL TOP

The dry tongues observed here are part of the entrainment process at the PBL top. It is important to estimate how large the entrainment is in this context and how its contribution and role evolves during the monsoon setting. One main issue that lies behind this is its possible importance in slowing down the monsoon with convective inhibition by drying the lowest troposphere, or favouring it by transporting humidity from the low troposphere to the mid-troposphere after it has been advected by the nocturnal jet.

Considering the linear shape of the observed heat flux profiles, and especially buoyancy, we can make estimates of entrainment buoyancy flux ratio β

$$\beta = -\frac{\overline{w\theta_v}|_i}{\overline{w\theta_v}|_0} \tag{1}$$

and entrainment velocity w_e

$$w_e = -\frac{\overline{w\theta_v}|_i}{\Delta\theta_v} \tag{2}$$

based on aircraft observations (Lenschow et al., 1999). $\overline{w\theta_v}|_i$ and $\overline{w\theta_v}|_0$ are the buoyancy flux at the PBL top and surface respectively and $\Delta\theta_v$ is the virtual potential temperature jump across the inversion ($\Delta\theta_v = \theta_v^+ - \theta_{v_m}$). The latter is deduced either from the radiosoundings made at Niamey at 1100 UTC or from an aircraft sounding. The buoyancy fluxes at PBL top and surface are extrapolated from the linear profile measured with the aircraft.

We find β=0.26 on average during the first period and β=0.13 during the second period. This means that entrainment is significantly smaller in the second period. Similarly, w_e is about 1.3 cms^{-1} in the first period while it

is only 0.4 cms^{-1} in the second. However, we find those estimates much smaller (about 5 times smaller) than we expected from the PBL growth $\frac{\partial z_i}{\partial t}$ that can be estimated from the UHF reflectivity profiles or the soundings made at different times of the day with balloons or airplane. Since

$$w_e = \frac{\partial z_i}{\partial t} - w_h, \tag{3}$$

our estimates of w_e from (2) should be of same magnitude of $\frac{\partial z_i}{\partial t}$, assuming the large scale velocity w_h is small.

There are several possible explanations for this: it is very difficult to estimate $\Delta\theta_v$ from soundings, because they often reveal a complex vertical structure, and above all, this structure can vary with time and space. It is especially difficult during the second period when clouds are present. However, neither errors that can be made on $\Delta\theta_v$ deduced from the soundings and on $\overline{w\theta_v}|_i$ deduced from the aircraft sampling, nor the large scale vertical velocity can explain such a difference between $\frac{\partial z_i}{\partial t}$ and w_e. A rapid variation of the flux profiles—although linearly varying with height—and of the structure of the entrainment zone (depth and scalar jumps) may be more responsible for it.

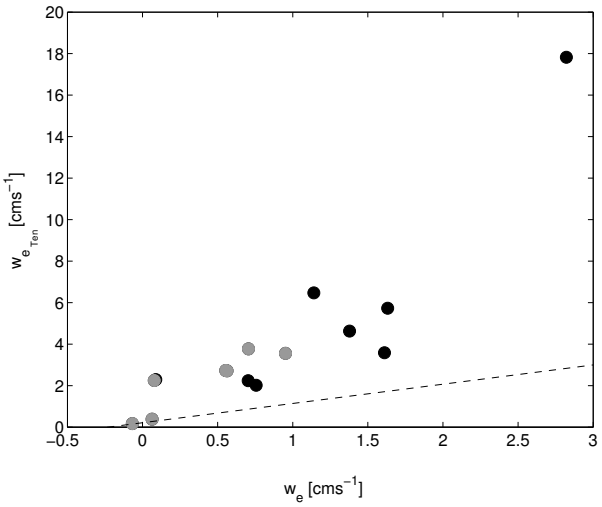

Figure 9: *Entrainment velocity as given by the mixed layer model of Tennekes (1973) versus the observed w_e. Again, the black and gray color stand for before and after the onset respectively.*

In Fig. 9, we compare our estimates of entrainment velocity with that predicted by the simple mixed-layer theory of Tennekes (1973), assuming a zero large scale velocity w_h:

$$w_{e_{Ten}} = (1+2\beta)\frac{\overline{w\theta}|_0}{\gamma z_i}, \tag{4}$$

where γ is the vertical gradient of θ_v in the free troposphere (SAL here). The discrepancy may be due to the uncertainty in estimating $\Delta\theta_v$ as pointed previously or γ. Also equation 4 does not take into account the contribution by shear at surface or at the top, even if they probably would not explain such a difference. A positive w_h would explain smaller entrainement velocity than observed PBL growth, but is rare. However, the context of the ITD convergence of dry static energy could be associated with large scale convergence overcapped above by the ITCZ subsidence branch. Considering equation 4 and our estimates of β, we find a contribution of entrainment to the total growth rate (which is equal to $2\beta/(1+2\beta)$) of 30% on average in the first period and less than 5% in the second. Our estimates of w_e are actually of the order of this contribution rather than the total.

During the first period, β takes a large spectrum of values from about 0 to 0.36 at maximum, so that it is neither constant nor equal to the typical value of 0.2 used in many models for the parameterisation of entrainment and closure at the PBL top. This can mean that the contribution of shear at surface and at the PBL top can vary from case to case.

Simple models (i. e. Mahrt and Lenschow, 1976) or recent parameterisations (i. e. Pino, 2006) of the contribution of shear at surface and shear at the top based on TKE budget integrated over the PBL depth did not lead to any convincing results, that is the theoretical contributions did not fit well to the observed entrainment. Meanwhile our observations based on aircraft-measured momentum fluxes and wind profiles show that the shear can be significant in the whole PBL, so that it does not generate TKE only close to the interfaces. Another unexpected result is that the wind shear at the PBL top, which is also difficult to estimate for the same reasons as $\Delta\theta_v$, is not well correlated to the latter. So we need further work on TKE budget using both the aircraft observations and LES to answer that question.

In spite of the limits encountered in explaining our estimates of entrainment at the interface between monsoon and Harmattan, we observe a good correlation between the latitudinal position of the ITD at 1200 UTC and our estimates of entrainment through w_e (Fig. 10) or β.

The ITD latitude position at Niamey longitude is calculated from the ECMWF analyses at 0.25° horizontal resolution, as the location of the maximum horizontal gradient of the 2 m dew point temperature. Because of turbulent mixing during the day, the position of the ITD at midday hours has a significant uncertainty, but it shows a consistent variability at the seasonal and diurnal scale (Lothon et al., 2008) and the correlation that we observe here is significant. Note that it is predominantly due to the correlation of the buoyancy flux at the PBL top and the ITD position. Thus the closer the ITD from the area, the larger the entrainment. Since the ITD is located more northward during the wet period and entrainment is smaller then,

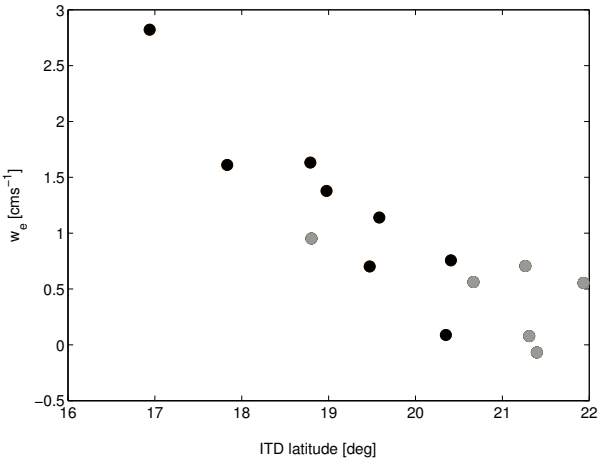

Figure 10: *Entrainment velocity as a function of the ITD position to the north of Niamey (black) before and (gray) after the onset.*

part of the correlation is built this way. But it is interesting to see that this correlation is very good (actually better) when considering only the flights made during the first period, that is when the ITD is still oscillating back and forth before setting further north at a more stable latitude. The amplitude of its latitudinal migration covers the spectrum of values for β.

6. SUMMARY AND PROSPECTIVES

When the depth of the PBL developing within the monsoon flow reaches the SAL, the entrainment at the top can have a very specific nature, with a large contribution of dry tongues to fluxes and other order moments down to at least 0.6 z_i. We made estimates of entrainment associated with them, characterized their scales and showed their impact in the vertical structure of the PBL. The impact of the entrainment processes down to surface is studied by a companion paper by Lohou et al. (2008).

We found larger entrainment in the first period than the second, and a large variability of the ratio of entrainment buoyancy flux over surface flux β.

A preliminary study of the link between the small scale exchanges at the ITD interface showed that the closer the ITD, the larger the entrainment at the sheared interface.

We still have to explain the large discrepancy between the observed entrainment velocity and the expected velocity from a rough theoretical estimate or from the observed PBL growth, because the uncertainty on the measured fluxes and scalar jumps cannot be the only explanation. An estimate of the large scale velocity within and above the SAL, in the area of the convergence zone of the ITD will be helpful.

We plan to further analyze the TKE budget along with the shear zone observed by the profilers in order to estimate the contribution of shear to entrainment. Also we showed different results between before and after the monsoon onset that are very likely due to the presence of clouds in the latter period. Those will be taken into account in our further analysis. The coupling of our observations with idealized LES will improve our understanding of those issues.

Acknowledgements

Based on a French initiative, AMMA was built by an international scientific group and is currently funded by a large number of agencies, especially from France, UK, US and Africa. It has been the beneficiary of a major financial contribution from the European Community's Sixth Framework Research Programme. Detailed information on scientific coordination and funding is available on the AMMA International web site http://www.amma-international.org. We thank the cooperation of the U.S. Department of Energy as part of the Atmospheric Radiation Measurement Program for processing the sounding data of Niamey site and for operating the UHF wind profiler in Niamey and providing the data. The authors of this work are funded by INSU-CNRS and Météo-France.

REFERENCES

Burpee, R. W., 1972: The origin and structure of easterly waves in the lower troposphere of North Africa, *J. Atmos. Sci.*, **29**, 77–90.

Couvreux, F., F. Guichard, J. L. Redelsperger, C. Kiemle, V. Masson, J. P. Lafore, and C. Flamant, 2005: Water-vapour variability within a convective boundary-layer assessed by large-eddy simulations and ihop-2002 observations, *Quart. J. Roy. Meteorol. Soc.*, **131**, 2665–2693.

Couvreux, F., F. Guichard, J. L. Redelsperger, and V. Masson, 2007: Negative water vapour skewness and dry tongues in the convective boundary layer: observations and LES budget analysis, *Boundary-Layer Meteorol.*, **123**, 269–294.

Lavaysse, C., C. Flamant, S. Janicot, D. J. Parker, J.-P. Lafore, B. Sultan, and J. Pelon, 2008: Seasonal evolution of the West African Heat Low: A climatological perspective, *Submitted to Clim. Dyn.*

Lebel, T., D. J. Parker, B. Bourles, C. Flamant, B. Marticorena, C. Peugeot, A. Gaye, J. Haywood, E. Mougin, J. Polcher, J.-L. Redelsperger, and C. Thorncroft, 2007: The AMMA field campaigns: Multiscale and multidisciplinary observations in the West African region, *Submitted to Ann. Geophys.*

Lee, Y., B. Campistron, and K. E. Kim, 2007: Preliminary results obtained from the 3d analysis of the amma wind-profiler radar synoptic network, *Second International AMMA Conference, Karlsruhe, 26-30 November 2007*.

Lenschow, D. H., P. B. Krummel, and S. T. Siems, 1999: Measuring entrainment, divergence and vorticity on the mesoscale from aircraft, *J. Atmos. Oceanic Technol.*, **16**, 1384–1400.

Lenschow, D. H., J. Mann, and L. Kristensen, 1994: How long is long enough when measuring fluxes and other turbulence statistics ?, *J. Atmos. Oceanic Technol.*, **11**, 661–673.

Lenschow, D. H. and P. L. Stephens, 1980: Rhe role of thermals in the convective boundary layer, *Boundary-Layer Meteorol.*, **19**, 509–532.

Lohou, F., F. Said, M. Lothon, P. Durand, D. Serca, D. Ramier, B. Cappelaere, and N. Boulain, 2008: Impact of the planetary boundary layer processes on the turbulent length scales and heat fluxes at surface, *Proceedings of 18th AMS Symposium on Boundary-Layers and turbulence, 9-13 June 2008, Stockholm, Sweden, American Meteorological Society, 45 Beacon ST., Boston, MA*.

Lothon, M., F. Couvreux, S. Donier, F. Guichard, P. Lacarrère, J. Noilhan, and F. Said, 2007: Impact of the coherent eddies on airborne measurements of vertical turbulent fluxes, *Boundary-Layer Meteor.*, **124, 425-447**.

Lothon, M., F. Said, F. Lohou, and B. Campistron, 2008: Observation of the diurnal cycle in the low troposphere of West Africa, *Mon. Wea. Rev., in press*.

Mahrt, L. and D. H. Lenschow, 1976: Growth dynamics of the convective mixed layer, *J. Atmos. Sci.*, **33, 41-51**.

Miao, Q. and B. Geerts, 2006: Vertical velocity and buoyancy characteristics of coherent echo plumes in the convective boundary layer, detected by a profiling airborne radar, *J. App. Meteorol. Clim.*, **45**, 838–855.

Nicholls, S., 1989: The structure of radiatively driven convection in stratocumulus, *Quart. J. Roy. Meteorol. Soc.*, **115**, 487–510.

Parker, D. J., R. R. Burton, A. Diongue-Niang, R. J. Ellis, M. A. Felton, C. M. Taylor, C. D. Thorncroft, P. Bessemoulin, and A. M. Tompkins, 2005: The diurnal cycle of the West African Monsoon circulation, *Quart. J. Roy. Meteorol. Soc.*, **131**, 2839–2860.

Peyrillé, P. and J. P. Lafore, 2007: An idealized two-dimensional framework to study the West African Monsoon. part II: Large-scale advection and the diurnal cycle, *J. Atmos. Sci.*, **64**, 2783–2803.

Pino, D., 2006: Role of shear and the inversion strength during sunset turbulence over land: characteristic length scales, *Boundary-Layer Meteorol.*, **121**, 537–556.

Sultan, B. and S. Janicot, 2000: Abrupt shift of the ITCZ over west africa, *Geophys. Res. Letter*, **27**, 3353–3356.

Sultan, B., S. Janicot, and P. Drobinski, 2007: Characterization of the diurnal cycle of the West African Monsoon around the monsoon onset, *J. Climate*, **20**, 4014–4032.

Tennekes, H., 1973: A model for the dynamics of the inversion above a convective boundary layer, *J. Atmos. Sci.*, **30**, 538–567.

Weckwerth, T., D. B. Parsons, S. E. Koch, J. A. Moore, B. B. Demoz, C. Flamant, B. Geers, J. Wang, and W. F. Feltz, 2004: An overview of the international h2o project (ihop_2002) and some preliminary highlights, *Bull. Amer. Meteorol. Soc.*, **85, 253-277**.